

**České vysoké učení technické v Praze
Fakulta elektrotechnická**

**Czech Technical University in Prague
Faculty of Electrical Engineering**

Doc. Ing. Stanislav Zvánovec, Ph.D.

Diverzitní techniky v bezdrátových optických sítích

Diversity techniques in free space optical networks

Summary:

Free space optics (FSO) offer many advantages for modern communication including larger frequency bandwidths and substantially higher available data rates, immunity to interference, free license, in addition to higher transmission safety. Recent transfers of air-to-ground quantum-key distributions at German Aerospace Center (DLR) and tests of optical links from the moon to NASA stations for future deep-space missions have proved challenging for this technology. However, FSO communications link performance is highly affected by the time-spatially variable turbulent environment and other atmospheric phenomena. To improve signal reception several mitigation techniques have been proposed and analytically investigated. To outline FSO prospects, this presentation introduces examples of analytical and experimental results for the route diversity technique utilization taken from research activities at the Czech Technical University in Prague.

The method describing the spatial influence of rainfall on microwave systems was adapted for optical links. The differences between both microwave and optical systems are discussed with regard to the newly derived dependences.

Most FSO links are deployed in dense urban areas, where thermal influences can be substantial. It is, therefore, beneficial to investigate the statistical influence of turbulences not only in open areas, but also in the vicinity of buildings. The next part deals with derivation of turbulence statistics for terrestrial and elevated links and diversity statistics from the outdoor measurement site of the Department of Electromagnetic Field. Following outdoor measurements, laboratory evaluations performed in cooperation with Northumbria University Newcastle are presented. Specific cases when several diversity links intersect a common turbulent area and each concurrently passes regions with different turbulence flows were analysed and a new model for joint diversity statistics was derived. A new laboratory for FSO link testing has been established at CTU.

The establishment of future optical wireless systems requires a full description of the dependences between atmospheric phenomena and the propagation channel. Although analytically and statistically based models for theoretical treatments of atmospheric influence on single FSO links were published, the experimental verifications together with statistics of wireless optical links are needed.

Souhrn:

Bezdrátové optické systémy (FSO) přináší řadu výhodných aspektů pro budoucí komunikační přenosy, jako je exténní šířka pásma umožňující vysokorychlostní přenos dat, imunita k interferencím, volný provoz aj. Poslední experimenty s přenosy kvantově distribuovaného klíče u spojů mezi pozemním segmentem a letadlem na DLR, či testy optického přenosu mezi stanicí na Měsíci a pozemními stanicemi NASA pro potřeby budoucích vesmírných misí prokazují vysoký potenciál této technologie. Nicméně jejich přenosové vlastnosti jsou ovlivněny časoprostorově proměnným médiem - atmosférou. Za účelem zlepšení přenosových statistik byla navržena a analyzována řada adaptivních technik.

Tato přednáška přináší konkrétní příklady analytických a experimentálních výsledků využití trasové diverzity u FSO systémů z vědecko-výzkumné činnosti na Katedře elektromagnetického pole ČVUT v Praze.

První část představuje implementaci metody prostorového vlivu deště z mikrovlnné oblasti u optických bezdrátových spojů. Jsou zde zdůrazněny rozdíly mezi těmito přístupy s ohledem na nově odvozené závislosti pravděpodobnosti zlepšení výpadků v optických sítích.

Vlivem toho, že většina současných FSO spojů je plánována do městských oblastí, kde dochází vlivem teplotní fluktuace k vzniku turbulencí v atmosféře, je nezbytné zkoumat vliv turbulencí na optické spoje. Další část přednášky se zabývá odvozením turbulentních statistik pro pozemní, letecké či družicové spoje a dále pak diverzitními statistikami z venkovního měřicího pracoviště Katedry elektromagnetického pole.

Pro upřesnění venkovních měření byly dále ve spolupráci s Northumbria University Newcastle provedeny laboratorní experimenty. Byly testovány speciální případy diversitních přenosů u diverzitních spojů protínajících jak společnou turbulentní oblast tak zároveň částečně v jiných místech ovlivňovaných rozdílnými turbulentními prouděními. Na základě experimentů byl odvozen nový model pro popis diverzitních statistik. Dále pak byla vytvořena nová laboratoř pro testování FSO spojů.

Závěrem je možné konstatovat, že pro rozvoj budoucích bezdrátových systémů je naprosto nezbytný plný popis vlivu přenosového prostředí na přenosový kanál. Přestože již byla analyticky a odvozena řada statistických modelů, experimentálních ověření jejich platnosti v širším kontextu je nezbytné.

Keywords: Free-space optical communication, diversity techniques, atmospheric turbulence, rain influence

Klíčová slova: Bezdrátové optické spoje, diverzitní techniky, atmosferická turbulence, vliv deště

Contents

1	Introduction	6
2	Analysis of influence of rain on FSO links	7
2.1	Join links route diversity	8
2.2	Diversity applied throughout the FSO network	10
3	Outdoor measurement of scintillation due to turbulence	11
3.1	Single link statistics measured at CTU	13
3.2	Vertical turbulence profiles	14
3.3	Diversity measurements	15
4	Indoor measurements	17
4.1	Separated channels	19
4.2	Open channels with partial correlation in turbulence	23
5	Conclusion and future work	27
	References	28
	Curriculum Vitae	33

1 Introduction

The time-variant influence of the atmosphere on Free-Space Optical (FSO) links [1] introduces a central drawback when this technology is used in place of slower (in terms of data rate) microwave links, or, in situations where there are no fibre optical links available [2]. The most significant concern in FSO systems and one which has been studied extensively in the literature is fog [3, 4]. Atmospheric thermal-induced turbulence is a second factor that notably impacts FSO link performance by affecting the statistics of the received signal [5]. The scintillations caused by variation in the reflective index due to the temperature and pressure fluctuations result in random variations of light intensities in both space and time at the receiver plane. In clear weather conditions, theoretical and experimental studies have shown that scintillation severely affects FSO link reliability and availability at all times [6, 7]. Scintillation has been extensively investigated and a number of theoretical models have been proposed to describe scintillation-induced fading [5, 7-9].

To overcome turbulence-induced fading in FSO systems, several techniques have been proposed including: spatial transmitter/receiver diversity [10] [11]; adaptive beamforming based on wavefront phase error measurement and settings of opposite phase aberration on the beam by a deformable mirror [12]; wavelength diversity [13], multiple-beam communication [14] and novel modulation techniques [15]. SIMO (single-input multiple-output) or MIMO (multiple-input multiple-output) optical channels have been studied for more than 40 years [16, 17] and measurements of SIMO systems have been reported in numerous papers, e.g. between a terrestrial station and satellite [18], ground station and aircraft [19], or, laboratory experiments [14, 20]. Approximations to the probability density function of the received power of a partial spatially correlated multiple-beam system have been proposed in relation to the single-channel gamma-gamma link function. A hybrid RF/optical link scheme [21, 22] offers almost 100% link availability and improved outage probability statistics, but at the cost of additional switching and buffering when using the RF link limiting the available data rates.

Error performance and the outage probability of a subcarrier intensity modulation (SIM) system employing the spatial and temporal diversity schemes to combat channel fading in the optical region were discussed in [23]. SIM with phase-shift keying (PSK) has been con-

sidered as an alternative for the turbulence-induced fading mitigation and can be applied in combination with spatial diversity [24]. In [24] the log-normal, gamma-gamma and negative exponential atmospheric turbulence models were extensively investigated and error performance in SIMO FSO links has been derived for three linear combining techniques: Maximal Ratio Combining (MRC); Equal Gain Combining (EGC); and, Selection Combining (SelC). It was shown that both multiple transmitter-single photodetector and single transmitter-multiple photodetector configurations employing EGC offer the same performance in turbulence conditions. The number of independent photodetectors capable of mitigating the scintillation without overwhelming complexity is reported to be approximately between two and four [24]. The subcarrier time delay diversity (TDD) was presented as an alternative technique for ameliorating channel fading and its error performance was analyzed in [23]. Retransmitting the delayed copy of the information just once was found to be the optimum with a gain of up to 4.5 dB in the weak atmospheric turbulence condition. The TDD gain was shown to be proportional to fading strength, but independent of data rate. Summarization of diversity techniques can be found in [25].

To support FSO performance analyses, as part of European COST (Cooperation in Science and Technology) action IC 1101 – OPTICWISE (Optical Wireless Communications – An Emerging Technology) [26], where our team active contributed, a common database of measuring sites, measured data and available software codes to has been developed to understand FSO problems and to derive theoretical and empirical models for single and diversity links. The goal of this presentation is to demonstrate the relationship between received optical power fluctuations, temperature gradients along the path of the optical beam caused by turbulence, rain influence and to highlight specific diversity approaches analysed and measured at the Czech Technical University in Prague (CTU) and Northumbria University Newcastle (NU).

2 Analysis of influence of rain on FSO links

The first part is devoted to the influence of rain on FSO links. To obtain precise fading statistics, the rain database from a four-year period, 2002-2005, was utilized including 250 km x 250 km rain scans from Czech meteoradars (rain rate distributions with 1 km grid resolution and 1-minute time steps).

2.1 Join links route diversity

To compare with previous results, examples are given for elevated platforms flying up to altitudes of 20 km. Methods for elevated links were adapted from a microwave region [27] with two evaluation methods tested based on simulation results: the first appropriated for isolated elevated systems and the second utilizing a combination of millimetre (frequency of 48 GHz) and Free Space Optical systems. The comparison of complementary cumulative distribution functions of rain attenuation for a single elevated platform to a user link at 48 GHz (ground distance 3 km) and for two branch diversity links at the same frequency where a user connects to two elevated platforms, can be seen in Fig.1. In the latter case, one of the two diversity links was identical to the standalone link and the second was angularly separated by 180 degrees with a land distance of 4.5 km.

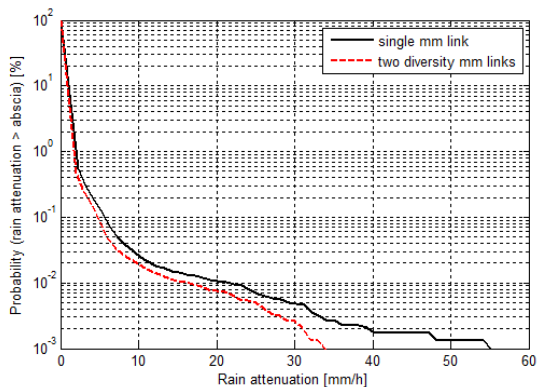


Figure 1: CDFs of rain attenuation for a single link and two-branch diversity links at 48 GHz with angular separation of 180 degrees and main and diversity ground link distances of 3 and 4.5 km

Resulting statistics for the same scenario, but with optical links, are depicted in Fig. 2. As can be clearly seen, both systems compensate, in similar ways, rain attenuation in terms of diversity gain. In the next step of our analysis, the performance of a single FSO link was tested for different elevation angles. See Fig. 3, where complementary cumulative distribution functions of a single FSO link are demonstrated for elevations of 90 degrees, 60 degrees and 45 degrees. Consequently,

statistics of elevated single FSO links were compared to rain attenuations between the same user and an elevated platform when the links used both parallel transmitted FSO and millimetre waves.

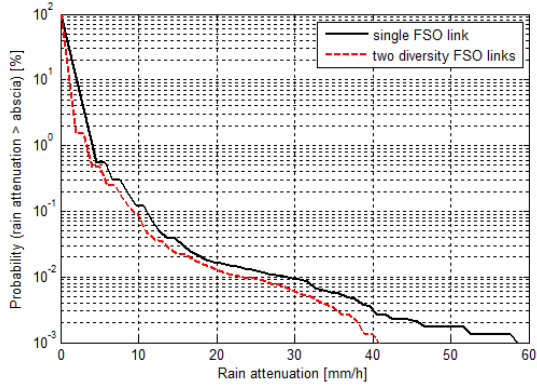


Figure 2: CDFs of rain attenuation for a single link and two-branch diversity elevated links at FSO wavelengths with an angular separation of 180 degrees and main and diversity ground link distances of 3 and 4.5 km

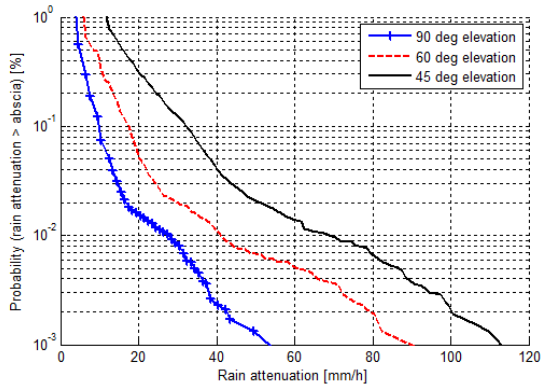


Figure 3: CDFs of elevated single FSO links influenced by rain

2.2 Diversity applied throughout the FSO network

Regarding whole system performance, the main analytical focus was to derive corresponding relations among rain event parameters and optical system availability, independent of the particular deployment of optical nodes and spatial distribution of users in the terrestrial network. Possible application of rainfall parameter, derived in [27] was tested even for an optical network. During heavy rainstorms, as expected, the network was capable of combatting undesirable rain attenuation by route diversity - by setting proper angular separations. Due to this approach, the outage improvement probability within the network increased by 11.4% (from 13.6% to 25.2%). This is an especially interesting indicator for the Czech Republic where a higher percentage of rain storms with smaller rain spatial parameters occurs.

An example of a comparison of outage improvement probability dependent on angular separations between diversity links and main to diversity link length ratios for a microwave terrestrial system working at a frequency of 48 GHz and wireless optical system is shown as follows in Fig. 4.

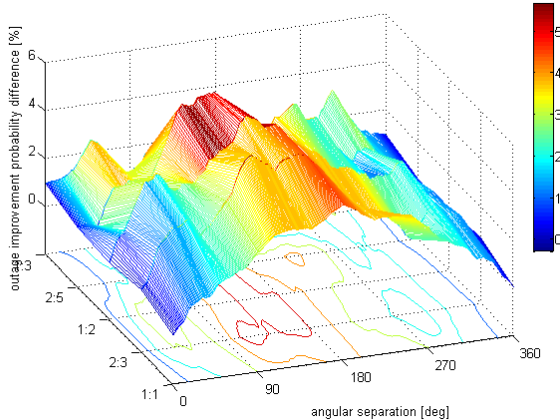


Figure 4: Example of comparison outage improvement probability [%] of microwave and optical networks

As can be seen in the optical network, higher outage improvement probabilities – varying between 1.6 and 5.3% - can be reached compared

to the RF network. In particular, the dependence of the a -parameter (for a thorough explanation see [27]) for higher rain intensities has a more rapid slope than in the case of 48 GHz. Outage improvements have been proved to have an exponential dependence on rain spatial parameters.

3 Outdoor measurement of scintillation due to turbulence

Scintillation and wandering of optical beams are mostly caused by thermal turbulence within the transmission medium and non-homogeneities of the refractive index. As air circulates within the urban environment, assuming temporal gradients from buildings and the ground, thermal characteristics can change dramatically along the optical link. Randomly distributed cells of different refractive indexes (so called eddies) can occupy areas ranging from a few centimetres up to units of kilometres [28]. The amplitude, as well as the frequency of received optical signal scintillations, is subsequently highly dependent on the turbulent cell size to beam diameter ratio. In this regard, an optical beam is deviated/bent in large turbulent areas, widened in a small turbulent area or, most typically, a combination of both mechanisms can be observed [28] (see illustration of the turbulent zones' influence on received optical power depicted in Fig. 5).

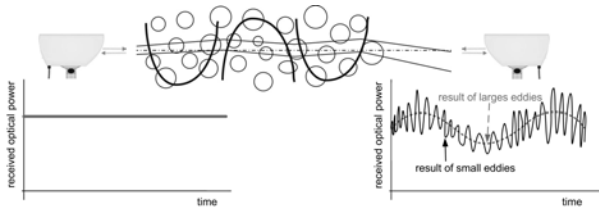


Figure 5: Demonstration of turbulence influence on FSO link

The frequency of received signal fluctuations can reach up to 200 Hz. The variance of scintillation (σ_χ^2) can be expressed by Rytov variance [29]

$$\sigma_\chi^2 = 1.23C_n^2 \left(\sqrt[6]{\left(\frac{2\pi}{\lambda}\right)^7 L^{11}} \right) \quad (1)$$

where λ represents the wavelength and L is the length of the link. C_n^2 introduces the so-called refractive index structure parameter- a vital measure of turbulence strength [30]. C_n^2 is a function of the wavelength, pressure and temperature changes as given by [28]:

$$C_n^2 = \left(86 \times 10^{-6} \frac{P_{as}}{T_e^2}\right)^2 C_T^2, \text{ at } \lambda = 850 \text{ nm} \quad (2)$$

where the temperature structure constant C_T^2 is related to the universal 2/3 power law of temperature variation as given in:

$$D_T = \langle (T_1 - T_2)^2 \rangle = \begin{cases} C_T^2 l_0^{-4/3} L_p^2 & \text{for } 0 < L_p < l_0 \\ C_T^2 L_p^{2/3} & \text{for } l_0 < L_p < L_0 \end{cases} \quad (3)$$

where T_1 and T_2 are the temperatures at two points separated by the distance L_p , l_0 and L_0 stand for the inner and outer scale of turbulence. Due to their random nature, turbulent media are extremely difficult to describe mathematically due to the presence of non-linear mixing of observable quantities [31]. Extensive research has been carried out, particularly in vertical variations of the structure parameter. For terrestrial sites (up to 100m of the Earth's atmosphere) the optical turbulence described by C_n^2 reaches values ranging from $10^{-17} \text{ m}^{-2/3}$ (weaker turbulence) to $10^{-13} \text{ m}^{-2/3}$ (stronger turbulence). According to [32], optical turbulence shows approximately diurnal cycles with peaks during midday hours and lowest values near sunrise and sunset. Several empirical models are utilized: The Hufnagel-Valley Model [32] for altitude and wind speed dependence; the Submarine Laser Communication-Day (SLC Day) model and the SLC Night model derived empirically from averaged measured data [33]; the Gurvich model for mid-scale turbulences etc.

Many statistical models were proposed to describe received signal fluctuations caused by atmospheric turbulence. Weak turbulences have been proved to have a probability density function (PDF) of the log-normal distribution [34] while for strong turbulences, the K-distribution [35] is used. Under the assumption that small-scale irradiance fluctuations are modulated by large-scale irradiance fluctuations of the propagating wave, gamma-gamma distribution can be utilized in a free space optical channel [36]. Several analyses of FSO bit error rate (BER) dependences on turbulence were accomplished in [35-39]. The method of turbulence mitigation was proposed in [40]. For more details on particular statistics see [41].

3.1 Single link statistics measured at CTU

To validate the influence of building heating effects on the free space optical link, an experimental campaign was set up at the campus of the Faculty of Electrical Engineering, Czech Technical University in Prague. Two free space optical transceivers WaveBridge 500 by Plaintree were placed on the roofs of two eight-story buildings on the CTU campus (see Fig. 6). This allowed us to build a 120-meter-long optical link at a wavelength of 850 nm, with transmitted power of 20 dBm. The data rate 150 Mbps (OC-3) was set in the link, while a router on one side returned back sent data. Data from two meteorological stations located in the middle of the link and one of the FSO transceivers, respectively, (see Fig. 6) were used for further analyses.

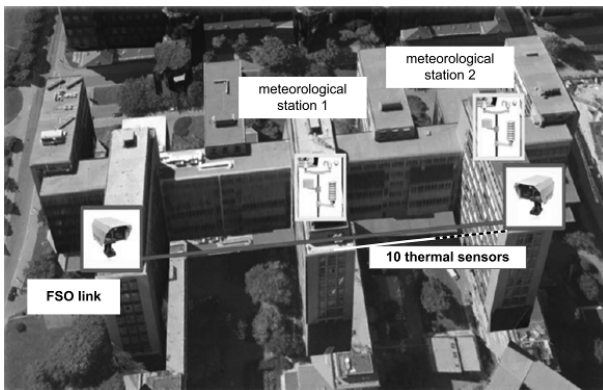


Figure 6: Deployment of the FSO link and weather sensors.

The temperature gradient was measured using a system of 10 thermal sensors equidistantly spaced along the first quarter of the free-space optical link [42]. In this way, thermal gradients are observed in various places around buildings, i.e. above the two buildings, and from close proximity to the building to a point halfway between both building wings. Samples of the dependency of received optical power and atmospheric parameters can be found in [1]. Based on statistics derived from sensor line measurements, the thermal influence of the buildings was analyzed. To validate the influences of the turbulent zones, the corrected dependence of the refractive index structure parameter was optimized from the Kolmogorov statistics of measured data [42]. From the measured data [42] it was seen that turbulence emerges approximately in

the first 1-2 meters surrounding the buildings (derived from a two-month measuring period). A high influence on the fluctuation of the received optical signals can be observed from turbulences arising up to 8 meters from the building. This is true especially during colder days, when the thermal heating of buildings radically changes the scintillation effects on a FSO link deployed in urban areas compared to links crossing free, non built-up areas.

3.2 Vertical turbulence profiles

The measured data from a 150-meter-high lattice mast located in Podebrady in the Czech Republic were used for the analysis of vertical profiles. Nineteen meteorological Vaisala HMP45D sensors, for temperature and relative humidity, were placed on the mast approximately 8 m from each other, between 5.11 m and 147.71 m above the ground.

Annual statistics of the refractive index structure parameter were generated separately at each height to form height profiles for the selected quantiles of 0.1%, 50%, 90%, and 99% of time and compared with the existing model (Hufnagel-Valley, SLC Day and Gurvich) - see Fig. 7. The adjusted parameters of models in the refractive index structure parameter were presented in [43].

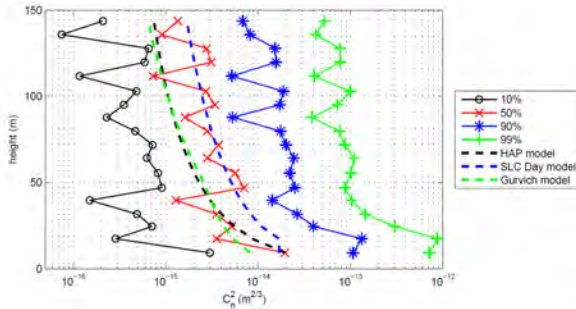


Figure 7: Measured refractive index structure parameter height profiles from May 2010 - April 2011 compared to models [43].

In addition, seasonal variations of the refractive index structure parameter were analysed - see results in Fig. 8. Drops in the winter refractive index structure parameter confirm a decrease in the average layer heights and air mass turbulent flows in cold months.

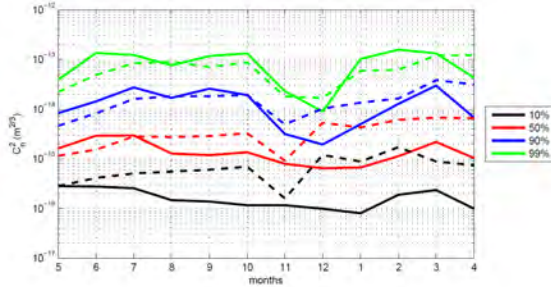


Figure 8: Fluctuations of the refractive index structure parameter over a one-year period at 39.71 m (solid lines) and 79.8 m (dashed lines) above the ground (May 2010 - April 2011)[43].

3.3 Diversity measurements

To fully comprehend turbulence phenomena for complex FSO networks, an original analysis of the influence of turbulence on the simple fragment of such a network with two route diversity links (from either two different distant points to the joint network node or in the reverse direction) had to be accomplished. In [44] the focus had been on the understanding of a route diversity concept from the point of view of turbulence scenarios and how they affected the performance of the FSO networks. In [45] another route diversity application for mesh optical networks was introduced together with interesting experiment results.

An experimental measuring network was set up at the university campus of the Czech Technical University in Prague (CTU). The network consisted of three FSO links (A - WaveBridge 500, B - Light-Pointe Strata G, C - MRV Telescope 700) and comprised a star topology network [46]. Arrangement of the network and sensors is depicted in Fig. 9. Weather conditions were observed by two meteorological stations. In the next step, the measuring network will be extended to a mesh topology by insertion of a new FSO link enclosing links B and C.

Data from FSO links A and B as a part of a star topology network was analyzed to investigate diversity statistics. To obtain these results, cumulative distribution functions (CDF) were analyzed and compared. All above-mentioned propagation impairments were dealt with and recalculated with regard to their spatial properties. Because of different link lengths, the diversity gain was recalculated to 1-km-long path.

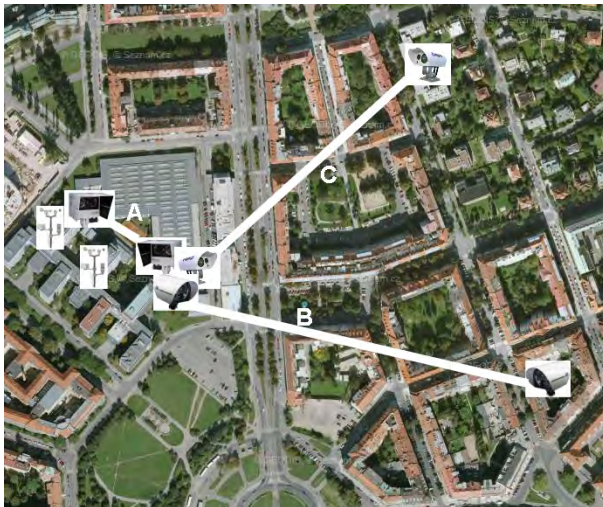


Figure 9: Measuring network and sensors' arrangement.

Table 1 shows the diversity gain of two FSO links derived from measured statistics during April and May 2011. As can be seen, diversity gains up to 8 dB are yielded. This contribution introduces every perspective possibility, especially within dense FSO networks during particular network segment (links) drops due to harsh atmospheric conditions [46].

For the analysis of the hybrid RF/FSO joint link, statistics measured by a 450- m-long link B between the CTU building and an Orlik dormitory were used. The free space link, consisting of a four-beam free space optical communication system FlightStrata G was equipped

Availability (%)	Diversity Gain Link A (dB)	Diversity Gain Link B (dB)
99.00	0.75	5.27
99.90	0.94	6.39
99.990	1.07	7.49
99.9990	1.27	8.36

Table 1: Selected diversity gains derived from statistics of two adjacent FSO links

with a backup RF link Mikrotik RB600A working at a frequency of 5 GHz. Deployment of both transceivers at the roof of the Orlik dormitory is depicted in Fig. 10.



Figure 10: a) FSO/RF transmitting site at the Orlik dormitory; b) experimental campaign arrangement for RF/FSO

The CDF of the joint hybrid RF/FSO link tends to be almost parallel to the CDF of the FSO in lower availabilities, but starts to diverge with availabilities higher than 99.7% (when diversity gain exceeds 17 dB). The highest outages were typically observed during foggy days.

4 Indoor measurements

Indoor laboratory atmospheric chambers have been developed at Northumbria University and recently at Czech Technical University (see Fig.11) to enable precise performance assessment of the FSO link under a controlled environment [5].

The indoor chamber offers the advantage of full FSO system characterization and investigation in much less time compared to outdoor FSO where it could take a long time for the weather conditions to maintain regular behaviour and changes that could not be accurately predicted, therefore, prolonging the characterization and measurements.

Example of the diversity measurement set-up tests using the NU laboratory atmospheric chamber is depicted in Fig. 12(a). Two narrow divergence beam laser sources, plus a collimated lens, were used at the transmitter side. The optical beams were modulated by a data source at a line-rate of 1 Mbit/s. The NU laboratory atmospheric channel

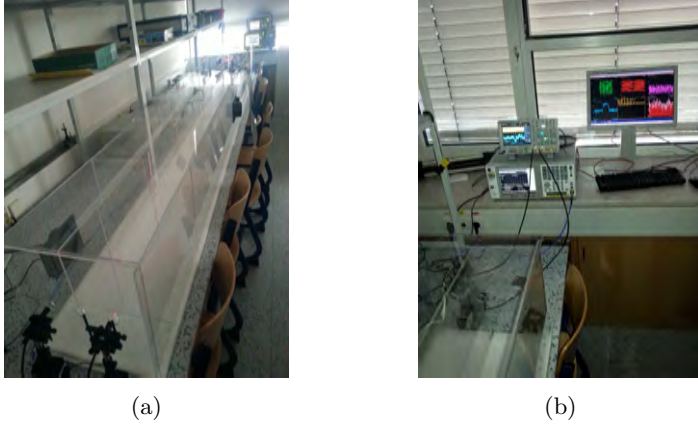


Figure 11: (a) New CTU turbulence chamber; (b) snapshot from 16-QAM FSO transfer measurement with turbulence influence.

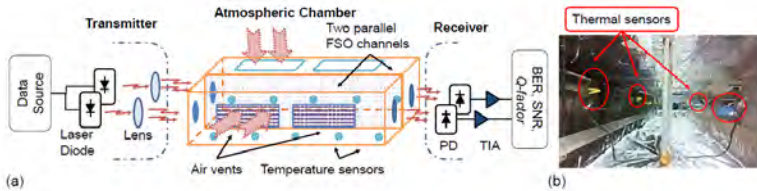


Figure 12: (a) Block diagram of the laboratory turbulence chamber; (b) snapshot of the deployment of thermal sensor line inside the chamber of NU [47].

is a closed glass chamber with dimensions of $5.5 \times 0.3 \times 0.3$ m and the chamber has air vents with external fans for air circulation along its length to control temperature distribution. External heaters were used to pump hot air into the chamber to create turbulence. There are also 19 remotely controlled thermal sensors positioned along the chamber to monitor and measure the temperature at one-second intervals with a resolution of 0.1 °C, see Fig. 12(b). The receiver front-end consists of a PIN photodetector and a transimpedance amplifier (TIA). The TIA output signal was captured using a wide bandwidth real time digital oscilloscope and a full signal analysis was carried out off-line in Matlab. The main parameters of the experimental system are given in [47].

4.1 Separated channels

The first testing measurement was performed using the Single-Input Multiple-Output transmission configuration. The laser beam at 830 nm was split into two halves, each propagating along a 1m channel separation in a non-turbulent and turbulent area, respectively, and then passing 1m of the common turbulent area (see Fig. 13a).

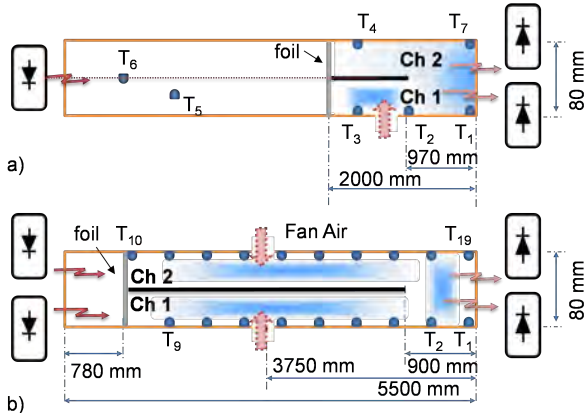


Figure 13: a) SIMO and b) MIMO FSO system under experimental laboratory set-up turbulence induced effect [49].

Since only small fraction of path was affected by turbulences, it resulted in a quite small scintillation effect. Diversity of these co-propagating beams varied around 0.2 dB and did not exceed 0.4 dB even in turbulences with $C_n^2 > 10^{-11} \text{m}^{-2/3}$. The effective area of the photodetector in one channel gave only small improvements ($\sigma_1^2(0)/\sigma_1^2(D) = 0.69$). The measured Rytov variance ratio between both receiving channels fluctuated from 0.9 to 0.15. This corresponds to the aperture averaging with $D = 5$ mm in the 5.5 m link and 30 mm in the 500 m link (see Fig. 14).

In the second case, channel 2 was influenced by constant weak turbulence (i.e. measured Rytov variance in the channel was kept less than 0.16). The turbulence circulating from channel 1 to the intersection area (and partially to the path of channel 1) was gradually increased from 10^{-13} to $10^{-11} \text{m}^{-2/3}$.

A decrease in the received power due to turbulences dependent of the mean index of refraction structure parameter measured along

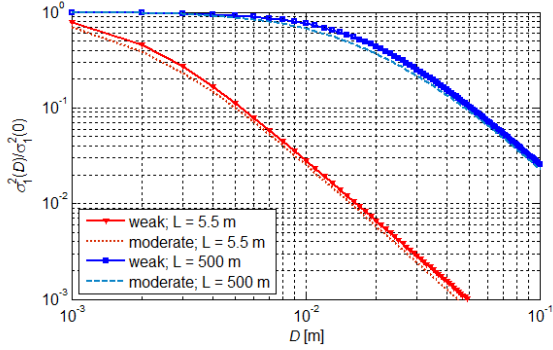


Figure 14: Aperture averaging derived for 5.5 m channel (red curves) and 500 m channel (blue curves) [49]

the channel 1 was experienced. Eye diagrams illustrated distortion in channel 1 which was affected by weak and moderate turbulences, as depicted in Fig. 15 and 16. Contrary to two co-propagated channels from the SIMO scheme for optical wireless links being separated at greater lengths and having common intersection turbulent area, measured scintillation was more than two orders higher. It has to be mentioned since the processed values of random variables (temperature distributions within the channels) were not strictly ergodic, so additional validations are needed. Extension of these measurements towards Ad-hoc networks was published in [49].

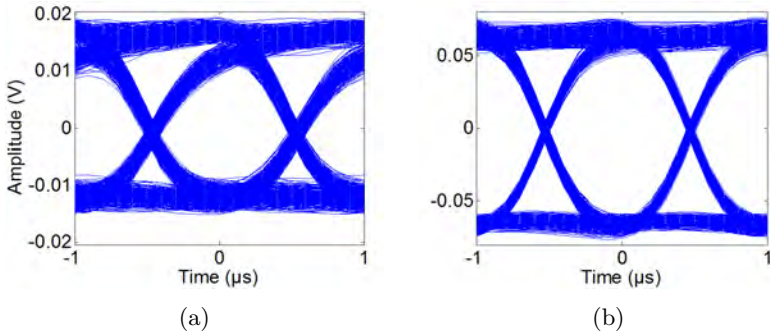


Figure 15: Eye diagram for initial turbulence scenario for received (a) channel 1 ($C_n^2 = 10^{-13} \text{ m}^{-2/3}$) and (b) chann. 2 received signals [49].

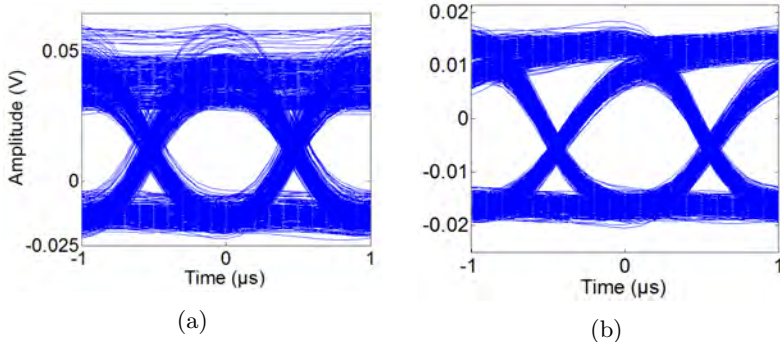


Figure 16: Eye diagram for final turbulence scenario for received (a) channel 1 ($C_n^2 = 10^{-11} \text{ m}^{-2/3}$) and (b) chann. 2 received signals [49].

A number of techniques have been proposed in the literature to deal with turbulence including aperture averaging, spatial diversity, and cooperative diversity, as mentioned in the introduction. As a first analysis, a pilot testing measurement was performed with multiple transmitters. Within the measured scenario, the laser beam at 830 nm was split into two with each beam propagating through two 1-m-long non-turbulent and turbulent channels and then through a 1-m-long common channel, see Fig. 17(a). The diversity scheme was evaluated via a diversity gain which is defined as the difference between attenuation of a single link and the minimum attenuation of joint diversity links.

To validate statistical results, the channel separation was increased and measurements were carried out over two separate channels isolated by a divider and foils. The measurement set-up within the turbulence chamber is shown in Fig. 17(b). Channel 2 was influenced by constant distortion or impairment due to the intensity variation of the received signal, i.e. with Rytov variance being kept below 0.09. This small intensity variation is not considered to be due to the turbulence, but rather more to do with the material used to isolate both channels. In this case the foil is a transparent film sheet made of polyethylene terephthalate or polyester, so the physical vibration of the foil is not significant to the human eye but does modify the intensity of the received signal, thus implying a small measured value of Rytov variance in the channel under study, however, this small deviation and variance is not associated with temperature effects. On the other hand, the turbulence in the channel 1 was gradually changed from low to moderate conditions.

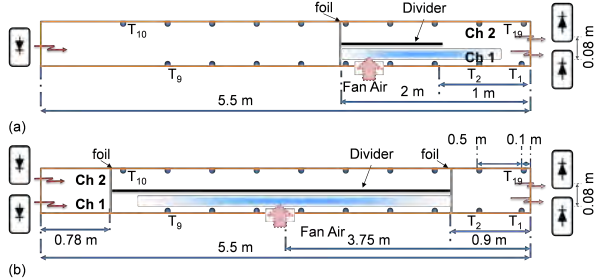


Figure 17: Deployment for measurement of two separated channels, (a) unique laser source SIMO and (b) dual laser source for isolated channel configuration [47].

In Fig. 18(a) Rytov variance derived both from the fluctuation of received optical signal and from the thermal sensors derived by integration over the thermal distribution using Eq. (5) for the same parameters are presented. Red circles show particular measurements for channel 1 with increased turbulence levels while the blue crosses represent parallel measurements for channel 2. Even though initially there was no turbulence in channel 2, we experienced some deviations in channel 2 due to the flow around the foils and the subsequent small vibration. As can be seen, the variance in optical signal increases even though there is no linear dependence with thermal variations within the channel.

Figure 18(b) gives insight to the ratio of the thermal structure and the refractive index structural parameters. Black dotted lines show theoretical C_n^2 dependence derived from Eq. (3) for the mean temperatures T_e 20°C and 40°C. Coloured lines, see inset, represent C_n^2 values enumerated from each sensor gap for all turbulence sets according to Eqs. (3) and (4), i.e. based on measured thermal differences and ensemble averaged values (channel 1 depicted in red solid line, channel 2 in blue dashed line) and C_T^2 . Finally, single points, red circles and blue crosses for channels 1 and 2, respectively, show the relations between two measured approaches - C_T^2 measured in channels via thermal distributions and C_n^2 observed through fluctuations of the received optical signal in terms of Rytov variance. C_n^2 values from three points of view are therefore compared: theoretical assumption, derivation from temperature fluctuations and enumeration of optical received fluctuations.

As can be seen, C_n^2 derived from thermal variation in turbulent con-

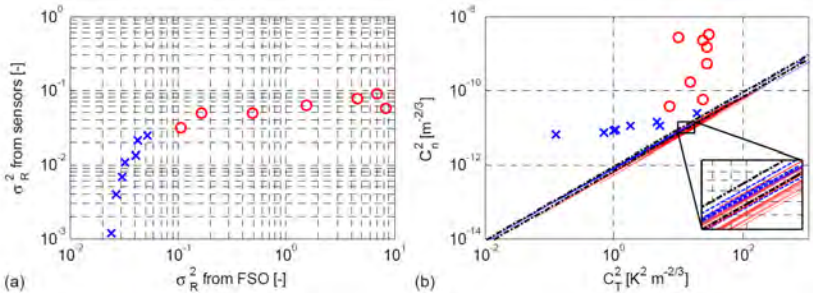


Figure 18: Measured dependence of (a) Rytov variances in both channels derived from received optical signal and from thermal sensor measurements (symbols, red circles - channel 1, blue crosses - channel 2) and (b) C_n^2 theoretical relations (black dotted lines), C_n^2 derived from measured thermal distributions via Eqs. (3) and (4) (channel 1 red and channel 2 blue lines) and C_n^2 derived from measured optical power on C_T^2 measured by the sensor line (symbols; red circles - channel 1, blue crosses - channel 2) [47]

ditions when particular sensor positions fully meet theoretical assumptions (coloured and black lines, respectively). For the distributions of C_n^2 , derived from Rytov variance, it is then evident that theoretical assumptions underestimate C_n^2 -to- C_T^2 ratio, which can be attributed principally to the integration over the link length to obtain C_T^2 .

4.2 Open channels with partial correlation in turbulence

When considering wireless network deployment in urban areas, the route diversity technique may be adopted to ensure higher link availability. To combat link failures FSO links can be arranged in several possible topologies thus offering diversity within the network to ensure link availability at all times.

The main aim during laboratory experiments was to analyze route diversity for two links when intersecting the same turbulent area (i.e. channel 2 and part of channel 1) with the fraction of the linearly increasing turbulent zone covering the major part of channel 1. This scenario corresponds to the real case when two links within the network terminate at the same point, i.e. passing the common volume

with the same or almost similar turbulence characteristic. Note, one of the optical links along the distant part is influenced by the non-correlated turbulent flow. The measurement deployment can be seen in Fig. 19.

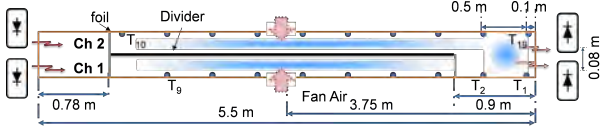


Figure 19: Deployment for measurement of partially correlated turbulences within channels [47].

Contrary to the previous case, the turbulence level in channel 2 was kept at a Rytov variance value of ~ 0.07 . Comparing the dependency of C_n^2 on C_T^2 (Fig. 5), we observed that there is a decrease in the slope for the moderate turbulence condition, see inset in Fig. 20. In the next step, the diversity gains were derived in relation to Q -factors of received OOK signal from off-line signal processing of both channels.

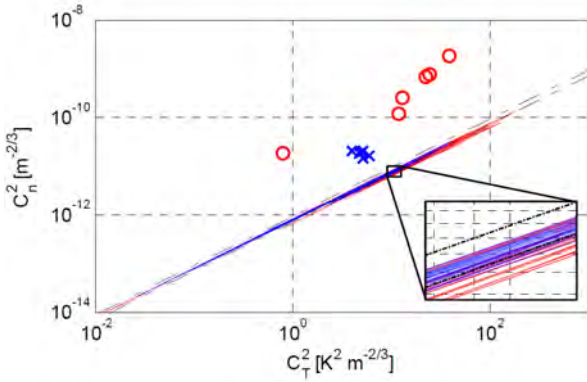


Figure 20: Dependence of C_n^2 derived from measured optical power (red circles – channel1, blue crosses - channel 2) and from the sensor line on the thermal structural parameter in partially correlated turbulences, temperature measurements from channel 1 (red solid lines) and channel 2 (blue dashed lines) line sensors, compared with C_n^2 dependence derived from Eqs. (3) and (4) for the mean temperatures of 20°C and 40°C (black dotted lines) [47]

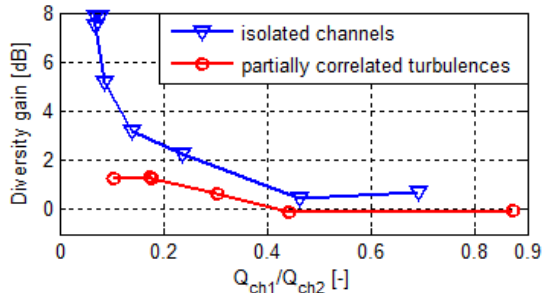


Figure 21: Comparison of diversity gains for two turbulence scenarios with respect to Q -factor ratio between channels [47]

The diversity gain against the Q -factor ratio between the channel with a low turbulence level and channels with high turbulence levels expressed by Q_{ch1}/Q_{ch2} is shown in Fig. 21. This Q -factor ratio expresses the relation of behaviour between both channels. Regarding Fig. 21, for two isolated channels, there is an obvious enhancement in the received power under a particular signal fade as the receiver can switch to the second (less affected) channel. This corresponds to similar characteristics derived analytically from the SelC diversity method [24]. To reduce the high processing load (thus the complexity) in SelC switched combining diversity, the switch-and-stay combining (SSC) and switch-and-examine combining (SEC) diversity schemes are introduced. In SSC, once the existing received SNR drops below a certain threshold level, the combiner switches to the next branch, regardless of SNR for the new branch, even if it is less than the original branch. In the SSC and SEC diversity schemes there is no need for continual monitoring of all receiving signals, thus leading to a much simplified receiver design compared to SelC [11, 48].

The SelC linear combiner samples the entire received signal through multiple branches and selects the branch with the highest SNR value or irradiance level, provided the photodetectors receive the same amount of background radiation. The output is equal to the signal on only one of the branches and not the coherent sum of the individual photocurrents as is the case in MRC and EGC. This makes SelC suitable for differentially modulated, non-coherent demodulated subcarrier signals. In addition, SelC is of reduced complexity compared to the MRC and

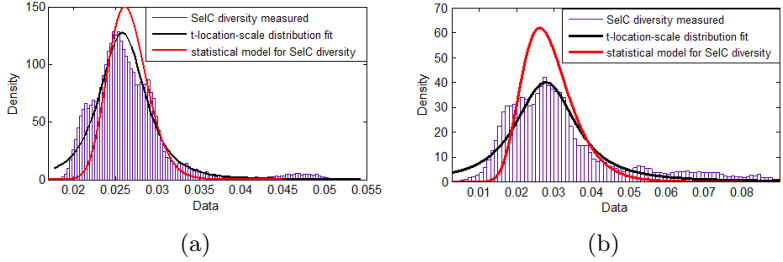


Figure 22: Examples from comparisons of measured and calculated Selection Combining diversity with Rytov variance in channels (a) $\sigma_1^2 = 0.03$, $\sigma_2^2 = 1.56$, (b) $\sigma_1^2 = 0.06$, $\sigma_2^2 = 5.42$ [47]

EGC and its conditional SNR is given by [24, 25]:

$$\gamma_{SelC}(I) = \frac{R^2 A^2 I_{max}^2}{2N\sigma} \quad (4)$$

where $I_{max} = \max(I_1, I_2, \dots, I_N)$. The pdf of the received irradiance, $p(I_{max})$, given by Eq. (5), is obtained by first determining its cumulative density function (cdf) and then differentiating.

$$p(I_{max}) = \frac{2^{1-N} N \exp(-y^2)}{I \sigma_i \sqrt{2\pi}} [1 + \operatorname{erf}(y)]^{N-1} \quad (5)$$

where

$$y = \frac{\ln(I/I_0) + \sigma_i^2/2}{\sqrt{2}\sigma_i} \quad (6)$$

From the measurements, it was observed that the above-mentioned analytical assumptions lead to an overestimation of received signal deviation in case of two channels crossing non-correlated turbulences. As can be seen in Fig. 22 from comparison of probability density functions of the measured route diversity data and the statistically derived PDF by Eq. (5), there is higher deviation in the measured selection diversity signal than expected. With increased turbulence levels in one of the channels we experienced heavier tails of pdf. Even though Eq. (5) in the majority of cases introduces quite a precise estimate, it was derived that the combined diversity statistics of the received route diversity signal follow the modified Student's t-distribution with N -degree of

freedom (corresponding to number of channels, i.e. in our case $N = 2$) described by the density function [47]:

$$p = \frac{\Gamma\left(\frac{N+1}{2}\right)}{\sigma\sqrt{N}\pi\Gamma\left(\frac{N}{20}\right)} \left[\frac{N + \left(\frac{I-I_0}{0.1\sigma}\right)^2}{N} \right] \quad (7)$$

Results from the second measurement set-up (see Fig. 19) indicate that the increment in transmitted optical power, or, switching to the second diversity link, has a reduced effect under the increased turbulence levels when both channels intersect a common turbulence area (red curve in Fig. 21). Comparison of the diversity gains with respect to the mean C_n^2 ratio between both the channels is given in Fig. 23. With increased turbulence level from low to moderate in channel 2, the system is more efficient with the route diversity scheme when both channels experience different turbulences along their links compared to the case when both links pass through a common turbulent channel.

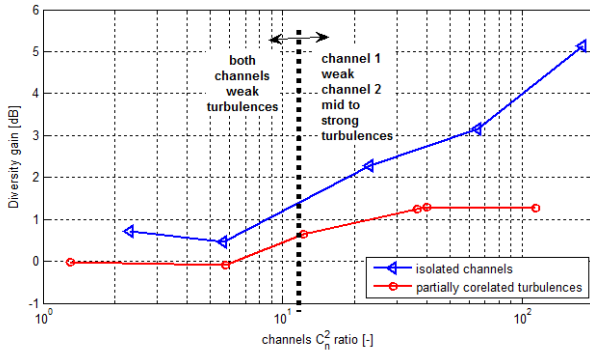


Figure 23: Comparison of diversity gains for two turbulence scenarios with respect to C_n^2 ratio between channels [47]

5 Conclusion and future work

The route diversity techniques for an FSO link were evaluated based on both the simulations and experimental work. We have focused on rain influence for joint links and whole affected network and, especially, on turbulence influence on diversity optical links. New results and models

were derived and published. The main aim was to find a description for a specific case where a number of diversity links experience both a common turbulent channel, and a channel with different turbulence regimes.

Joint international research is focused to the characterization of scintillation index, eye diagrams and structure coefficient statistics within an ad-hoc FSO networks and hybrid FSO/submillimeter band networks. The derived results from test scenarios demonstrated that it could be more effective to adopt the aperture averaging scheme than using multiple receiver to reduce the influence of turbulence on propagating optical beam through the shortest paths. On the contrary for the fades of segments where the majority of link paths experience different turbulence regimes, the fluctuations of received signals can be substantially reduced by retransmitting the information over the diversity path.

Based on the original measurement results more complex system analyses will be performed in upcoming research projects. CTU team will be focused on the complex Ad-hoc networks within action IC 1101 – OPTICWISE (Optical Wireless Communications – An Emerging Technology) and Visible Light Communications (VLC), where the team just now perform several joint research campaigns in cooperation with Northumbria University, Newcastle upon Tyne (team of prof. Ghassemloooy), Politecnico di Milano (team of prof. Capsoni), University of the Negev (team of prof. Arnon) and other research laboratories and industrial partners. Joint EU Horizon2020 project has been prepared towards these technologies.

References

- [1] O. Bouchet, *Free-space optics : propagation and communication*. London ; Newport Beach, CA: ISTE, 2006.
- [2] J. Perez, et al., "Ethernet FSO Communications Link Performance Study Under a Controlled Fog Environment," *IEEE Communications Letters*, vol. 16, pp. 408-410, 2012.
- [3] M. Grabner and V. Kvicera, "The wavelength dependent model of extinction in fog and haze for free space optical communication," *Opt. Express*, vol. 19, pp. 3379-3386, 2011.
- [4] J. Perez, et al., "Ethernet FSO communications link performance study under a controlled fog environment," *IEEE Commun. Lett.*, vol. 16, pp. 408-410, Mar 2012.

- [5] Z. Ghassemlooy, et al., "Performance analysis of ethernet/fast-ethernet free space optical communications in a controlled weak turbulence condition," *J. Lightwave Technol.*, vol. 30, pp. 2188-2194, Jul 1 2012.
- [6] Z. Xiaoming and J. M. Kahn, "Performance bounds for coded free-space optical communications through atmospheric turbulence channels," *IEEE Trans. Commun.*, vol. 51, pp. 1233-1239, 2003.
- [7] W. Gappmair, "Further results on the capacity of free-space optical channels in turbulent atmosphere," *IET Commun.*, vol. 5, pp. 1262-1267, 2011.
- [8] M. A. Khalighi, et al., "Fading reduction by aperture averaging and spatial diversity in optical wireless systems," *IEEE/OSA J. Opt. Commun. Networking*, vol. 1, pp. 580-593, 2009.
- [9] T. A. Tsiftsis, et al., "Optical wireless links with spatial diversity over strong atmospheric turbulence channels," *IEEE Trans. Wireless Commun.*, vol. 8, pp. 951-957, 2009.
- [10] S. M. Navidpour, et al., "BER performance of free-space optical transmission with spatial diversity," *IEEE Trans. Wireless Commun.*, vol. 6, pp. 2813-2819, Aug 2007.
- [11] H. Moradi, et al., "Switch-and-stay and switch-and-examine dual diversity for high-speed free-space optics links," *IET Optoelect.*, vol. 6, pp. 34-42, 2012.
- [12] R. K. Tyson, "Bit-error rate for free-space adaptive optics laser communications," *J. Opt. Soc. Am. A*, vol. 19, pp. 753-758, 2002.
- [13] V. Weerackody and A. R. Hammons, "Wavelength Correlation in Free Space Optical Communication Systems," in *Proceedings of IEEE Military Comm. Conf.*, 2006, pp. pp. 1-6.
- [14] J. A. Anguita, et al., "Spatial correlation and irradiance statistics in a multiple-beam terrestrial free-space optical communication link," *Appl. Opt.*, vol. 46, pp. 6561-6571, Sep 10 2007.
- [15] N. D. Chatzidihamantis, et al., "Adaptive subcarrier PSK intensity modulation in free space optical systems," *IEEE Trans. Commun.*, vol. 59, pp. 1368-1377, May 2011.
- [16] Rosenber.S and M. C. Teich, "Photocounting Array Receivers for Optical Communication through Lognormal Atmospheric Channel" *Applied Optics*, vol. 12, pp. 2625-2635, 1973.
- [17] A. Belmonte, et al., "Atmospheric-turbulence-induced power-fade statistics for a multiaperture optical receiver," *Applied Optics*, vol. 36, pp. 8632-8638, Nov 20 1997.
- [18] M. Jeganathan, et al., "Data analysis results from the GOLD experiments," *Free-Space Laser Communication Technologies*, vol. 2990, pp. 70-81, 1997.

- [19] F. G. Walther, et al., "Air-to-Ground Lasercom System Demonstration Design Overview and Results Summary," *Free-Space Laser Communications X*, vol. 7814, 2010.
- [20] E. J. Lee and V. W. S. Chan, "Part 1: Optical communication over the clear turbulent atmospheric channel using diversity," *IEEE Jour. on Sel. Areas in Comm.*, vol. 22, pp. 1896-1906, 2004.
- [21] N. Letzepis, et al., "Outage analysis of the hybrid free-space optical and radio-frequency channel," *IEEE J. Sel. Areas Commun.*, vol. 27, pp. 1709-1719, Dec 2009.
- [22] L. Eunju, et al., "Performance analysis of the asymmetric dual-hop relay transmission with mixed RF/FSO links," *IEEE Photonics Technol. Lett.*, vol. 23, pp. 1642-1644, 2011.
- [23] W. O. Popoola, et al., "Error performance of terrestrial free space optical links with subcarrier time diversity," *IET Comm.*, vol. 6, pp. 499-506, 2012.
- [24] W. O. Popoola, et al., "Free-space optical communication employing subcarrier modulation and spatial diversity in atmospheric turbulence channel," *IET Optoelectron*, vol. 2, pp. 16-23, 2008.
- [25] W. Popoola, Z. Ghassemlooy, S. Zvanovec, "Diversity, Networking and Redundancy," in Handbook of Measurements, *COST IC0802 Final Report*, A. Martellucci, Ed., ed, 2013.
- [26] "COST action IC 1101 OPTICWISE", retrieved 1.10.2013, <http://opticwise.uop.gr/>.
- [27] S. Zvanovec and P. Pechac, "Rain spatial classification for availability studies of point-to-multipoint systems," *IEEE Transactions on Antennas and Propagation*, vol. 54, pp. 3789-3796, Dec 2006.
- [28] L. C. Andrews and R. L. Phillips, *Laser beam propagation through random media*, second ed. Washington: SPIE Press, 2005.
- [29] A. Al-Habash, et al., "Comparison between experimental and theoretical probability of fade for free space optical communications," *Proc. Conf. Optical Wireless Communications V*, 2002.
- [30] A. Kolmogorov, Ed., *Turbulence (Classic Papers on Statistical Theory)*. New York: Wiley-Interscience, 1961, p.pp. Pages.
- [31] G. R. Osche, *Optical detection theory for laser applications*, 1 ed.: Wiley-Interscience, 2002.
- [32] L. C. Andrews, *Field guide to atmospheric optics*, 1st ed. Bellingham, Wash.: SPIE Press, 2004.
- [33] M. Miller and P. L. Zieske, "Turbulence environmental characterization," *RADC-TR-79-131, ADA072379*,, 1976.
- [34] X. Tang, et al., "Performance of BPSK Subcarrier Intensity Modulation Free-Space Optical Communications using a Log-normal Atmospheric Turbulence Model," *The Int. Symp. on Photonics and Optoelec.*, Chengdu, China, 2010.

- [35] H. Samimi and P. Azmi, "Subcarrier Intensity Modulated Free-Space Optical Communications in K-Distributed Turbulence Channels," *Journal of Opt. Comm. and Networking*, vol. 2, pp. 625-632, Aug 1 2010.
- [36] M. Uysal, et al., "Error rate performance analysis of coded free-space optical links over gamma-gamma atmospheric turbulence channels," *IEEE Transactions on Wireless Communications*, vol. 5, pp. 1229-1233, Jun 2006.
- [37] L. Han, et al., "Performance of free space optical communication through gamma-gamma turbulence channels with spatial diversity," *Conf. on Computer and Comm. Techn.*, Chengdu, 2010.
- [38] A. Jurado-Navas, et al., "Efficient lognormal channel model for turbulent FSO communications," *Electronics Letters*, vol. 43, pp. 178-180, Feb 1 2007.
- [39] H. E. Nistazakis, et al., "Average Capacity of Optical Wireless Communication Systems Over Atmospheric Turbulence Channels," *Journal of Lightwave Technology*, vol. 27, pp. 974-979, 2009.
- [40] M. A. Khalighi, et al., "Turbulence Mitigation by Aperture Averaging in Wireless Optical Systems," *Proc. of the 10th Int. Conf. on Telecomm. Contel 2009*, Zagreb, Croatia, June 2009.
- [41] L. C. Andrews, et al., *Laser beam scintillation with applications*, Bellingham, Wash.: SPIE Press, 2001.
- [42] J. Libich and S. Zvanovec, "Influences of turbulences in near vicinity of buildings on free-space optical links," *IET Microwaves Antennas and Propagation*, vol. 5, pp. 1039-1044, Jun 27 2011.
- [43] O. Jicha, P.Pechac, S. Zvanovec, M. Grabner, V. Kvicera, "Long-term measurements of refractive index structure constant in atmospheric boundary layer," *SPIE Conf.*, 2012.
- [44] A. Kashyap, et al., "Integrated topology control and routing in wireless optical mesh networks," *Computer Networks*, vol.51, pp. 4237-4251, 2007.
- [45] S. Kaneko, et al., "Evaluation of a free-space optical mesh network communication system in the Tokyo metropolitan area," *J. Opt. Netw.*, vol. 1, pp. 414-423, 2002.
- [46] J. Libich, et al., "Mitigation of time-spatial influence in free-space optical networks utilizing route diversity," *Free-Space Laser Communication Technologies Xxiv*, vol. 8246, 2012.
- [47] S. Zvanovec, J. Perez, Z. Ghassemlooy, S. Rajbhandari, J. Libich, "Route diversity analyses for free-space optical wireless links within turbulent scenarios," *Optics Express*, vol. 21, pp. 7641-7650, 2013.
- [48] K. Young-Chai, et al., "Analysis and optimization of switched diversity systems," *IEEE Trans. Veh. Technol.*, vol. 49, pp. 1813-1831, 2000.

- [49] J. Perez, S. Zvanovec, Z. Ghassemlooy, W. O. Popoola, Experimental characterization of mitigation of turbulence induced signal fades within an ad-hoc FSO network, *Optics Express*, submitted for publication.
- [50] K. Young-Chai, et al., "Analysis and optimization of switched diversity systems," *IEEE Trans. Veh. Technol.*, vol. 49, pp. 1813-1831, 2000

Curriculum Vitae

doc. Ing. Stanislav Zvánovec, Ph.D.

Date of birth: January 29, 1977

Education and Academic Qualifications:

- 2010 Assoc. Professor (doc.), CTU in Prague, in Radioelectronics.
- 2006 PhD degree, CTU in Prague, in Radioelectronics.
- 2002 MSc (Ing) degree, CTU in Prague, in Radioelectronics.

Employment:

- Assistant Professor, Dept. of Electromagnetic Field FEE CTU Prague (2005-2010)
- Associate Professor, Dept. of Electromagnetic Field FEE CTU Prague (since 2010)
- Head, Freespace and nonlinear fiber optics, Department of Electromagnetic Field FEE CTU Prague (since 2008)
- Visiting research fellow, Northumbria University, Newcastle upon Tyne, 2012
- Visiting research fellow, Politecnico di Milano, 2013

Grants, Research Projects:

- Research within fields of wireless optics, fiber optics and propagation of electromagnetic waves in the frame of international projects ESA PECS no. 98069, ESA 4000105298/12/NL/CLP, COST projects IC1101, IC0802, IC0603, Centre for quasi-optical systems and terahertz spectroscopy KVASTES, projects TACR TA01011105 (obtained 2013 prize of TACR for originality of the solution), TACR grant TA03010060, GACR P206/10/2182, 102/08/P346, IRP projects of MEYS a numbers of project NBU.

Professional Societies, Boards and Committees:

- IEEE - chair of Joint MTT/AP/ED/EMC Chapter of the Czechoslovakia Section.

- URSI - F Commission (Wave Propagation and Remote Sensing) Chair for Czech republic
- COST IC 1101 (OPTICWISE - Optical Wireless Communications - An Emerging Technology) - vice-chair WG1 (Propagation Modelling and Channel Characterization)
- Editorial board of impacted journal Radioengineering
- Local Organizing Chair of European Conference on Antennas and Propagation EuCAP 2012 and member of TPC of many other conferences (ISMOT 2011, XXIX General Assembly of URSI, Radioelektronika, COMITE. . .)
- Reviewer selected journals - Optics Express, Journal of Lightwave Technology, IEEE Transactions on Antennas and Propagation, IEEE Antennas and Wireless Propagation Letters, Journal of The Franklin Institute-engineering and Applied Mathematics. . .

University Courses:

- Measurement of Fiber Optical Communications (A0M17MVK)
- Optical Communication Systems (A2B17OKS)
- Fiber Optics Detection (A0M17VOD)
- Perspectives in Millimetre and Submillimetre Technology (A0M17TMS)
- Terrestrial and Satellite Radio Links (A0M17PDS)
- Fixed and Mobile Wireless Links (A02B17PMS)

PhD supervision.

- From 1996 till 2003 co-supervised 3 PhD students at the Czech Technical University in Prague (two successfully defended their thesis, last submitted thesis in Sept. 2013). At CTU in Prague 2 PhD students supervised by S. Zvanovec will defend PhD theses 9th Jan 2014. Currently supervising 5 PhD students. Since February 2013 has been S. Zvanovec as chairperson of ORO (Branch Board) of PhD branch 2601V010 Radioelectronics.

Selected Publications:

(most publications available on-line at zvanovec.elmag.org).

- P. Pechač, S. Zvánovec, „Základy šíření vln pro plánování pozemních rádiových spojů“, 1. vyd. Praha: BEN - technická literatura, 2007, 200 s. ISBN 978-80-7300-223-7.
- P. Piksa, S. Zvánovec, P. Černý, „Specific Millimeter-Wave Features of Fabry-Perot Resonator for Spectroscopic Measurements“, in book „Microwave and Millimeter Wave Technologies: from Photonic Bandgap Devices to Antenna and Applications” edited by I. Minin, Vukovar: In-Teh, 2010, p. 451-468. ISBN 978-953-7619-66-4.
- S. Zvanovec, J. Perez, Z. Ghassemlooy, S. Rajbhandari, J. Libich, „Route diversity analyses for wireless optical links within turbulent scenarios”, Optics Express, vol. 21, Issue 6, pp. 7641-7650, 2013.
- M. Písařík, P. Peterka, S. Zvánovec, Y. Baravets, F. Todorov, I. Kašík, P. Honzátko „Fused fiber components for „eye-safe“ spectral region around 2 micrometers“, Optical and Quantum Electronics, accepted for publication, 2013.
- J. Libich, S. Zvánovec, „Influences of Turbulences in Near Vicinity of Buildings on Free Space Optical Links“, IET Microwaves, Antennas and Propagation, 2011, vol. 5, issue 9, p. 1039 - 1044.
- P. Černý, P. Piksa, S. Zvánovec, T. Kořínek, V. Kabourek, „Improved Axial Excitation of Fabry-Perot Resonator for High Resolution Spectroscopy Applications“, Microwave and Optical Technology Letters. 2011, vol. 53, no. 11, p. 2456-2462. ISSN 0895-2477.
- M. Komanec, P. Honzátko, S. Zvánovec, „Single-shot all-optical sampling oscilloscope using a polarization-maintaining resonator for pulse replication“, Microwave and Optical Technology Letters. 2010, vol. 52, no. 11, p. 2452-2456. ISSN 0895-2477.
- S. Zvánovec, P. Pechač, „Validation of Rain Spatial Classification for High Altitude Platform Systems”, IEEE Trans. on Antennas and Propagation, 2011, vol. 59, issue 7, p. 2746-2750.

- S. Zvánovec, P. Pechač, „Rain Spatial Classification for Availability Studies of Point-to-Multipoint Systems”, IEEE Transactions on Antennas and Propagation, vol. 54, no. 12, 2006. pp. 3789-3796.
- M. Polívka, M. Švanda, P. Hudec, S. Zvánovec, „UHF Radiofrequency Identification of People in Indoor and Open Areas”, IEEE Transactions on Microwave Theory and Techniques, volume 57, Issue 5, Part 2, pp.1341-1347, May 2009.
- S. Zvánovec, P. Černý, P. Piksa, T. Kořínek, P. Pechač, et al., „The use of the Fabry-Perot interferometer for high resolution microwave spectroscopy“, Journal of Molecular Spectroscopy. 2009, vol. 256, no. 1, p. 141-145. ISSN 0022-2852.